Electroluminescence and Photophysical Properties of Polyquinolines

Xuejun Zhang, Ashok S. Shetty, and Samson A. Jenekhe*

Departments of Chemical Engineering and Chemistry, University of Rochester, Rochester, New York 14627-0166

Received June 16, 1999; Revised Manuscript Received September 7, 1999

ABSTRACT: The electroluminescence and photophysical properties of a series of 11 polyquinolines were investigated and used to explore the effects of molecular and supramolecular structures on the light-emitting properties of polymers. Thin films of the polyquinolines have photoluminescence quantum yields between 2 and 30% and unusually long excited-state lifetimes of 2.4−5.2 ns. Electroluminescence colors spanning blue, green, yellow, orange, and red were obtained through regulation of the molecular and supramolecular structures of the excimer- and aggregate-forming polyquinolines. ITO/hole transport layer/polyquinoline/Al light-emitting diodes fabricated and evaluated in air had electroluminescence quantum efficiencies between 0.02 and 1% and luminance levels of up to 280 cd/m^2 at a current density of 100 mA/cm^2. The electroluminescence efficiency approximately scaled linearly with the photoluminescence quantum yield. Favorable reaction at the aluminum/polyquinoline interface is proposed to account for the efficient electron injection and device performance in spite of the large (1.5−1.9 eV) energetic barrier to electron injection. These results provide new insights into the design of efficient light-emitting polymer materials and devices for optoelectronic applications.

Introduction

Semiconducting polymers with efficient electroluminescence are being developed for various lighting and flat-panel display applications.[1] A better understanding of the relationships of electroluminescence (EL) and photophysical properties of polymers to molecular and supramolecular structures is critical to the rational design of polymers with enhanced EL properties and device performance. Poly(*p*-phenylenevinylene) (PPV), polythiophene (PT), poly(*p*-phenylene) (PPP), polyfluorene, and their derivatives have been extensively investigated as emissive materials for EL devices.[1] Although a systematic variation of the side group attached to the polythiophene backbone has been shown to tune the EL color from blue to the near-infrared, the materials generally have very low luminescence quantum yield.[2] PPV-based materials have high photoluminescence (PL) and EL efficiencies, and the EL color can be varied by side-chain substitutions and copolymerizations.[1] However, degradation induced by photooxidation,[3] which may impede long-term device stability, is a concern with arylenevinylene polymers. Furthermore, all these extensively studied PPV-, PPP-, PT-, and polyfluorene-based EL materials are *p-type* semiconductors with very good *hole* transport but very poor *electron* transport properties.[1−4]

Luminescent polymers with efficient electron injection and transport properties are of interest in their own right as well as to complement existing p-type polymers for the development of more efficient EL devices. Such *n-type* (electrons transport) polymers offer alternative EL device engineering compared to p-type polymers.[5] Here, we focus on the EL and photophysical properties of the polyquinolines which are known to be intrinsic n-type semiconducting polymers. Their n-type characteristics were revealed in previous studies by chemical doping,[6] ion implantation,[7] photoconductivity,[8] and electrochemical redox measurements.[9] The polyquinolines also have excellent mechanical properties and high thermal stability and can be processed into high-quality thin films.[10,11] They were also shown to have interesting

Chart 1

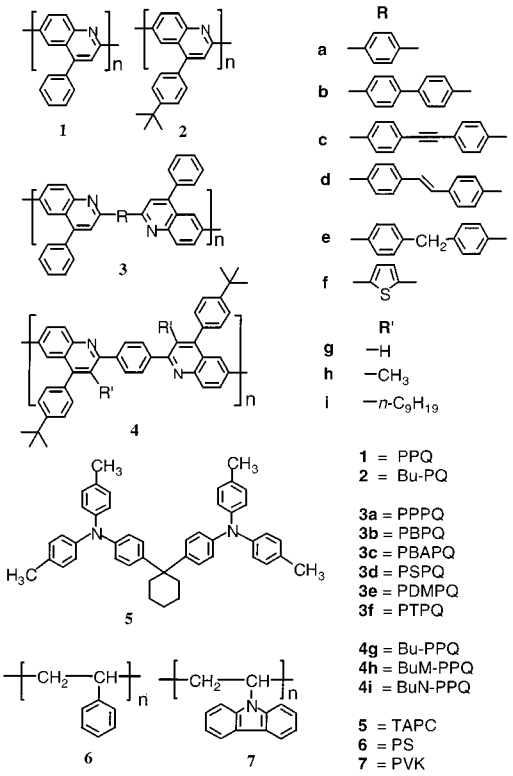

electronic,[11] photoconductive,[8] and nonlinear optical[12] properties. Recently, some polyquinolines were demonstrated as promising materials for the fabrication of light-emitting diodes (LEDs).[5b,c,13,14] However, their EL and photophysical properties have not been systematically investigated.

This paper reports studies of the electroluminescence and associated photophysical properties of a series of 11 polyquinolines with different molecular structures. As shown in Chart 1, variation in the polyquinoline backbone linkage (R) and pendent side groups provided

10.1021/ma990960+ CCC: $18.00
Published on Web 10/14/1999

a means to regulate the intramolecular and supramolecular structures which in turn substantially influenced the observed optoelectronic properties and EL device performance. From the results we conclude that the n-type polyquinolines are promising emissive materials for efficient and bright light-emitting devices whose colors can be tuned throughout the visible from blue to red.

Experimental Section

Materials. The synthesis, characterizations, thin film processing, optical absorption, electrochemistry, and nonlinear optical properties of polymers **1** and **3a**−**f** were previously reported by our group.[8,9,11,12] The synthesis and characterizations of polymers **2** and **4g**−**i** were also reported in previous communications.[14] The polyquinolines used in this study have intrinsic viscosities of 0.74−31.3 dL/g, which were measured in 0.1 mol % di-*m*-cresyl-phosphate/*m*-cresol at 25 °C or in methanesulfonic acid at 30 °C.[11,14] The exact molecular weights of these polymers are unknown. However, light scattering measurements on **3b** gave a weight-average molecular weight (M_w) of 370 000 for a sample with an intrinsic viscosity of 20 dL/g.[15] The above intrinsic viscosity values of the polyquinolines used in this study indicate that they are moderate to high molecular weight polymeric materials. 1,1-Bis(di-4-tolylaminophenyl)cyclohexane (TAPC) was provided by Eastman Kodak Co. Polystyrene (PS) with a molecular weight (M_n) of ∼200 000 and poly(vinylcarbazole) (PVK) (M_n = 100 000) were obtained from Polysciences. The chemical structures of all the materials used in this study are shown in Chart 1.

Thin Film Processing. Optical quality thin films of the polyquinolines were obtained by spin-coating from their formic acid solutions. All polymer solutions were filtered with 0.2 μm Acrodisc 13 CR PTFE syringe filters (Pall Corp., East Hills, NY) prior to spin-coating. Films for optical absorption and photoluminescence measurements were spin-coated onto silica substrates. All the films were dried overnight at 60 °C in a vacuum.

UV−vis and Photoluminescence Spectroscopies. Optical absorption spectra were obtained by using a Lambda-9 UV/vis/near-IR spectrophotometer (Perkin-Elmer). Steady-state photoluminescence studies were carried out by using a Spex Fluolog-2 spectrofluorimeter. The films for steady-state PL studies were positioned such that the light emission was detected at 22.5° from the incident beam. The PL quantum efficiencies of polymers were estimated by using a thin film of ∼10^{-3} M 9,10-diphenylanthracene in poly(methyl methacrylate) as a standard (ϕ_{PL} = 83%).[16,17]

$$\phi_x = \phi_r\left(\frac{I_x}{I_r}\right)\left(\frac{E_r}{E_x}\right)\left(\frac{A_r}{A_x}\right)\left(\frac{n_x}{n_r}\right)^2 \quad (1)$$

where the *x* and *r* subscripts refer to the sample of unknown PL quantum yield and the standard, respectively. ϕ is the PL quantum efficiency, *I* is the integrated PL intensity, *E* is the monochromatic excitation intensity, *A* is the fraction of the excitation light absorbed by the sample, and *n* is the refractive indices of the sample. Refractive indices for the standard and the unknown were assumed to be close, and no corrections were made. *A* can be approximated by the absorbance (<0.1) since all films were optically thin. The *E* term correction can be eliminated by using Rhodamine B as an internal standard so that the PL spectra were taken in the ratio (*s*/*r*) mode. *I* was calculated from the recorded PL spectrum.

Electrochemistry. Electrochemical (redox) properties of the recently synthesized polyquinolines (Bu-PQ, Bu-PPQ, BuM-PPQ, and BuN-PPQ) were investigated by cyclic voltammetry (CV). Platinum (Pt) wire electrodes were used as both counter and working electrodes, and the Ag/Ag^+ electrode was used as the reference. Polymers were coated onto the working electrode by dipping the Pt wire electrodes into viscous polymer solutions. CV measurements were done in an electrolyte solution of 0.1 M tetrabutylammonium hexafluorophosphate (Bu_4NPF_6) in acetonitrile. The detailed experimental procedures were the same as previously reported.[9]

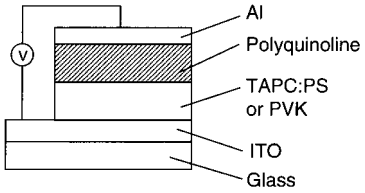

Figure 1. Schematic structure of LED fabricated from polyquinoline thin films.

Photoluminescence Decay Dynamics. Time-resolved photoluminescence decay measurements were performed by using the time-correlated single photon counting technique.[22b,c] The excitation system consists of a cavity pumped dye laser (Coherent model 703D) circulating rhodamine 6G, synchronously pumped by a mode-locked frequency doubled Nd:YAG laser (Quantronics model 416). The dye laser pulses were typically 10 ps duration at a repetition rate of 38 MHz, and the samples were excited at 350 nm. The PL decay was detected at the PL emission peak for each polymer.

LED Fabrication and Characterization. Electroluminescent devices were prepared and investigated as sandwich structures between aluminum and indium−tin oxide (ITO) electrodes (Figure 1). The ITO glass substrates were purchased from Donelley (Holland, MI). TAPC dispersed in polystyrene (TAPC:PS) or PVK was used as the hole-transport layer (HTL) since polyquinolines are n-type semiconducting polymers. PVK was only used for BuM-PPQ and BuN-PPQ devices. Thin films (50 nm) of TAPC:PS (50 wt %) or PVK were deposited onto ITO coated glass substrates by spin-coating from dichloromethane solutions. Thin films (30−60 nm) of conjugated polyquinolines were spin-coated from their formic acid solutions onto the TAPC:PS or PVK layer and dried at 60 °C in a vacuum overnight. The film thicknesses were measured by an Alpha-step profilometer (Tencor Northern) with an accuracy of ±1 nm and confirmed by an optical absorption coefficient technique. Finally, 100−130 nm aluminum electrodes were vacuum (5×10^{-6} Torr) evaporated onto the resulting bilayers. The area of each EL device was 0.2 cm^2. Electroluminescence spectra were obtained by using a Spex Fluorolog-2 spectrofluorimeter. Current−voltage (*I*−*V*) and luminance−voltage curves were recorded simultaneously by hooking up an HP4155A semiconductor parameter analyzer (Yokogawa Hewlett-Packard, Ltd., Tokyo) together with a Grasby S370 optometer (Grasby Optronics, Orlando, FL) equipped with a calibrated luminance sensor head.

The EL quantum efficiencies of the diodes were measured by using procedures similar to those previously reported.[18] Photons emitted from LEDs were detected with a calibrated Grasby 221 photodiode (350−1100 nm, built into a Grasby 2550 integrating sphere). The photocurrent (I_{ph}) was converted to a voltage signal by the S370 optometer and subsequently recorded by the HP4155A semiconductor parameter analyzer,

$$I_{ph} = \frac{V}{G} \quad (2)$$

where *V* is the measured voltage (V), and *G* is the gain (V/A) set for the S370 optometer. Since the photocurrent was caused by the photons emitted from the LED, we have

$$I_{ph} = \int N(\lambda)\,\frac{hc}{\lambda}\,i(\lambda)\,d\lambda = \frac{V}{G} \quad (3)$$

where λ is the wavelength of the photons, $N(\lambda)$ is the emission rate of photons at wavelength λ, hc/λ is the photon energy, and $i(\lambda)$ is the responsitivity of the photodiode (A/W). Letting N_{ph} be the total emission rate of photons from the LED and $n(\lambda)$ the fraction of photons with wavelength λ, we have

$$n(\lambda) = \frac{N(\lambda)}{N_{ph}} \quad (4)$$

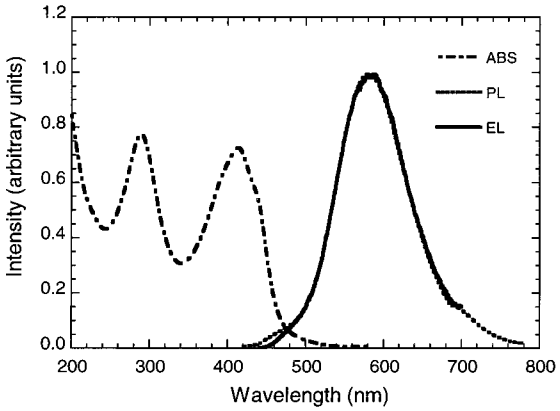

Figure 2. Optical absorption, PL (400 nm excitation), and EL (at 10 V) spectra of PPQ (**1**).

The fraction $n(\lambda)$ was calculated from the EL spectrum with the normalization condition

$$\int n(\lambda)\, d\lambda = 1 \tag{5}$$

Therefore, the total number of photons emitted from an LED per second is obtained from

$$N_{ph} = \frac{V}{G\int n(\lambda)\frac{hc}{\lambda} i(\lambda)\, d\lambda} \tag{6}$$

From the recorded current (I) passing through the LED, the total number of electrons injected into the polymer per second is

$$N_e = \frac{I}{e} \tag{7}$$

Therefore, the EL quantum efficiency (photons/electron) of the LED can be obtained from

$$\phi_{EL} = \frac{N_{ph}}{N_e} \tag{8}$$

Such a measured EL efficiency is the external efficiency. The internal EL quantum efficiency was obtained by multiplying the external efficiency by the factor of $2n^2$ where n is the refractive index of the emissive polymer.[18] We used 1.6 as the refractive index n of the polyquinolines[11b] in our estimations of the internal EL efficiency. All the LED fabrication and evaluation were done under ambient laboratory conditions.

Results and Discussion

A. Photophysical Properties. Optical Absorption Spectra. The optical absorption spectrum of a thin film of the parent polyquinoline PPQ (**1**) is shown in Figure 2. The $\pi-\pi^*$ transition has a lowest energy absorption maximum (λ_{max}) at 414 nm and an absorption edge (E_g^{opt}) of 2.65 eV. Representative optical absorption spectra of several polyquinolines (BuM-PQ, PDMPQ, Bu-PPQ, PPPQ, and PTPQ) are shown in Figure 3. The lowest energy transitions in the absorption spectra and estimated optical gaps of all the polyquinolines investigated are collected in Table 1. The optical absorption spectra revealed that most of the polyquinolines (PPQ, Bu-PQ, PPPQ, Bu-PPQ, PBPQ, PBAPQ, and PSPQ) have similar $\pi-\pi^*$ transitions with λ_{max} at 399−414 nm (Table 1). The $\pi-\pi^*$ transition showed a gradual small red shift, suggesting increasing electron delocalization along the chain as the linkage changed from phenylene (**3a**, PPPQ) to biphenylene (**3b**, PBPQ), ethynylenebiphenylene (**3c**, PBAPQ), and acetylenebiphenylene (**3d**, PSPQ). The most striking red shift was observed in PTPQ with the thienylene linkage (**3f**), showing the $\pi-\pi^*$ absorption maximum at 471 nm compared to 400 nm for PPPQ (**3a**). On the other hand, PDMPQ (**3e**) in which the conjugation was disrupted by a methylene linkage showed a blue shift (380 nm) in absorption maximum compared to the case of PPPQ.

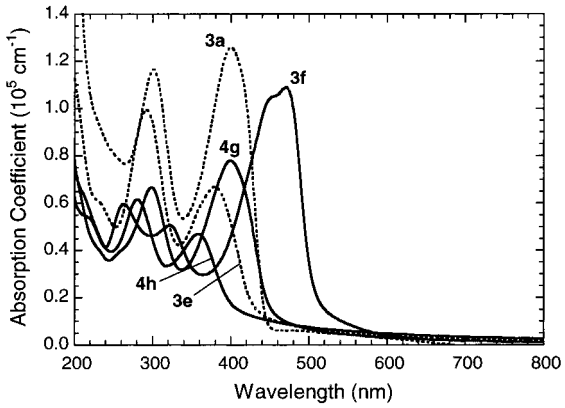

Figure 3. Optical absorption spectra of thin films of representative polyquinolines: BuM-PPQ (**4h**), PDMPQ (**3e**), Bu-PPQ (**4g**), PPPQ (**3a**), and PTPQ (**3f**).

Table 1. Optical Absorption and Redox Properties of Polyquinoline Thin Films

polymer	λ_{max}, nm	α,[a] 10^5 cm^{-1}	E_g^{opt},[b] eV	E^{red},[c] V	E^{ox},[c] V
1, PPQ	414	1.12	2.65	−1.78	0.95 (0.87)[d]
2, Bu-PQ	412	0.69	2.65	−1.86	0.78 (0.79)
3a, PPPQ	400	1.31	2.78	−1.90	1.07 (0.88)
3b, PBPQ	405	1.17	2.81	−1.98	1.09 (0.83)
3c, PBAPQ	407	1.12	2.72	−1.93	1.08 (0.79)
3d, PSPQ	414	1.13	2.65	−1.92	0.95 (0.73)
3e, PDMPQ	380	0.67	3.01	−2.04	1.04 (0.97)
3f, PTPQ	471	1.09	2.49	−1.84	0.87 (0.65)
4g, Bu-PPQ	399	0.78	2.78	−1.58	0.99 (1.20)
4h, BuM-PPQ	358	0.47	3.10	−1.95	1.35 (1.15)
4i, BuN-PPQ	347	0.44	3.26	−2.00	1.31 (1.26)

[a] Data for solid films at absorption λ_{max}. [b] Optical absorption edge gap (E_g^{opt}). [c] Onset potentials vs SCE from ref 9, except for **2** and **4g**−**i**. [d] E^{ox} determined from $E^{ox} = E_g^{opt} - |E^{red}|$.

Introduction of *tert*-butyl substitution on the phenyl side group does not appear to affect the ground-state electronic structure of the polyquinolines as seen by comparing the absorption spectra of PPQ to Bu-PQ (**2**), PPPQ, and Bu-PPQ (**4g**). Bu-PQ has essentially the same absorption peak (412 nm) as PPQ (414 nm). Bu-PPQ (**4g**) has an identical absorption peak and edge as PPPQ (**3a**). However, substitution of methyl or nonyl side groups to the bis(quinoline) rings caused large changes in the electronic structure of the polymer. BuM-PPQ (**4h**) and BuN-PPQ (**4i**) have absorption λ_{max} at 358 and 347 nm, respectively, which are substantially blue-shifted from the parent Bu-PPQ (**4g**) with absorption peak at 399 nm (Table 1). These effects of methyl and nonyl substitutions indicate that electron delocalization is disrupted along the chain. We can understand these optical absorption spectra and their dependence on main-chain and side-group variations in terms of the effects of geometric structure on the ground-state electronic structure of the polyquinolines. Similar effects of intramolecular and supramolecular interactions on the photophysical properties of oligoquinolines have been found in oligomers investigated by single-crystal X-ray diffraction.[19] From the oligoquinoline crystal struc-

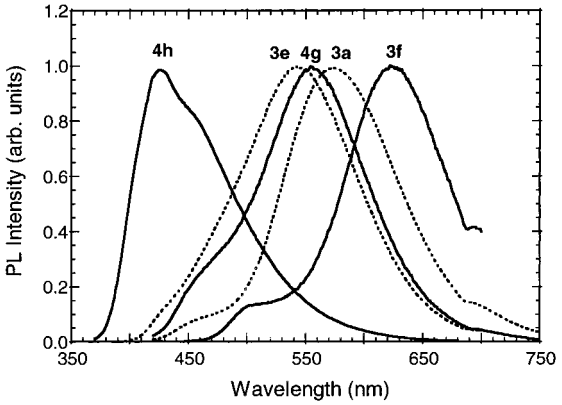

Figure 4. PL spectra of thin films of polyquinolines: BuM-PPQ (**4h**), PDMPQ (**3e**), Bu-PPQ (**4g**), PPPQ (**3a**), and PTPQ (**3f**). The polymers were excited at their absorption peaks.

Table 2. PL and EL Properties of Polyquinoline Thin Films

polymer	λ_{max}^{PL},[a] nm	ϕ_{PL}, %	λ_{max}^{EL}, nm	h,[b] nm	V_{on}, V	luminance/I/V, cd/m^2, mA/cm^2, V	ϕ_{EL}, %
1, PPQ	578	10	589	30	7	130/235/17.5	0.46
2, Bu-PQ	571	20	586	60	9	100/80/22	0.92
3a, PPPQ	574	10	580	50	9	70/145/20	0.46
3b, PBPQ	571	9	557	30	7	60/500/15	0.15
3c, PBAPQ	564	9	554	35	7	114/500/16	0.20
3d, PSPQ	590	3	585	35	7	26/270/15	0.10
3e, PDMPQ	542	12	534	35	7	60/60/15	0.92
3f, PTPQ	622	2	622	40	5	10/500/12	0.02
4g, Bu-PPQ	554	30	554	50	8	280/100/20	1.08
4h, BuM-PPQ	425	8	426	45	11[c]	7/55/20	0.15
4i, BuN−PPQ	424	9	410	33	10[c]	15/100/19	0.15

[a] PL obtained by exciting at absorption λ_{max}. [b] h = film thickness of polyquinoline in EL devices. [c] All LED data for HTL = TAPC except for **4h** and **4i** where HTL = PVK.

tures[19] it is clear, for example, that a twist angle exists between the plane of the bis(quinoline) rings and the plane of the aromatic R linkage. The twist angle varied with the R moiety and also with the 3,3′-alkyl substitutions on the bis(quinoline) rings.[19]

In addition to the lowest energy optical transition whose λ_{max} and absorption edge (E_g^{opt}) are listed in Table 1, a second higher energy absorption band was commonly observed in most of the polyquinolines. In the case of the basic polyquinoline PPQ (**1**), the higher energy peak at 290 nm (Figure 2) actually has a slightly larger oscillator strength than the lowest energy band at 414 nm. The ratio of the oscillator strength of the lowest energy transition to that of the higher energy transition was found to vary with molecular structure as exemplified in Figure 3. The absorption coefficient α at the lowest energy λ_{max} shown in Table 1 also varies considerably with polyquinoline structure. We anticipate that the excited-state properties of the polyquinolines will be similarly regulated by molecular structure.

Photoluminescence. The thin film photoluminescence (PL) spectrum of the basic polyquinoline PPQ (**1**) is also shown in Figure 2. This polymer has a PL peak at 578 nm, emitting orange light. Shown in Figure 4 are representative PL spectra for BuM-PPQ (**4h**), PDMPQ (**3e**), Bu-PPQ (**4g**), PPPQ (**3a**), and PTPQ (**3f**), which have PL emission peaks at 426, 534, 554, 574, and 622 nm, respectively. The thin film PL peaks and PL efficiencies of all the polyquinolines are listed in Table 2. The steady-state PL spectra thus show that the emission colors of the polyquinolines can be tuned from blue (BuM-PPQ and BuN-PPQ) to green (PDMPQ), yellow (Bu-PPQ), orange (PPQ, Bu-PQ, PPPQ, PBPQ, PBAPQ, and PSPQ), and red (PTPQ).

By comparing the optical absorption and PL spectra of the polyquinolines, it can be seen that polyquinolines **1**, **2**, **3a**−**f**, and **4g** have large Stokes shifts of 160−180 nm, which is characteristic of excimer emission of solid films of many conjugated polymers.[20] On the other hand, polyquinolines **4h** and **4i** have much smaller Stokes shifts (67−77 nm). All the polyquinolines have broad, featureless, emission bands that are also characteristic of excimers or aggregates.[20] From the previously cited single-crystal X-ray diffraction structures of oligoquinolines, it is known that the corresponding polymers such as PPPQ (**3a**) and PTPQ (**3f**) have essentially planar backbone structures with an intermolecular face-to-face distance of ∼3.5 Å.[19] In contrast, similar oligomer data indicate that BuM-PPQ (**4h**) and BuN-PPQ (**4i**) have nonplanar chain structures and relatively large intermolecular distances of ∼10 Å.[19b] We can conclude that the solid-state emission of most of the polyquinolines (**1**, **2**, **3a**−**f**, **4g**) originates from excimers. The emission bands of BuM-PPQ (**4h**) and BuN-PPQ (**4i**), however, we tentatively assign to emission from ground-state intermolecular aggregates in view of the relatively large intermolecular distances of their oligomers.[19]

Most of the polyquinolines, including **3a**−**e**, have solid-state PL efficiencies of about 10%, which is similar to the parent polyquinoline PPQ (**1**). The two blue-emitting polymers BuM-PPQ (**4h**) and BuN-PPQ (**4i**) with apparent aggregate emission also have PL efficiencies comparable to those of PPQ (**1**). However, two polyquinolines with *tert*-butyl substitutions (Bu-PQ and Bu-PPQ) have higher PL efficiencies (20−30%) compared to those of related polymers without *tert*-butyl substitutions. It is remarkable that the side-group *tert*-butyl substituents in Bu-PQ (**2**) and Bu-PPQ (**4g**) result in factors of 2 and 3 enhancements in PL quantum efficiency compared to those of the parent polymers PPQ (**1**) and PPPQ (**3a**), respectively, with only minor emission spectral shifts. This suggests that although the basic excited-state electronic structure of **1** and **3a** is only slightly modified by such a substitution, the changes in intermolecular packing in **2** and **4g** relative to **1** and **3a** dramatically reduce quenching of emission yield. That the luminescence efficiency of conjugated polymer thin films could be controlled by side-chain substituents or copolymerization which regulates chain packing or intermolecular interactions was previously suggested in a broader context[20] but only demonstrated in random rod/coil copolymers.[17] The fact that the PL efficiencies of BuM-PPQ (**4h**) and BuN-PPQ (**4i**) are similar to that of PPPQ (**3a**) but substantially lower than that of Bu-PPQ (**4g**) clearly shows that some side-group substitutions are more effective than others in enhancing luminescence efficiency through control of intermolecular interactions. From the present results we see that those side-group substitutions which also cause significant main-chain twisting, as in BuM-PPQ and BuN-PPQ, are least effective. The reason for this appears to be that the twisting of the main chain of the conjugated polymer can induce a large change in the ground-state and excited-state electronic structures of the fluorescent polymer.

Among all the polyquinolines, PSPQ (**3d**) and PTPQ (**3f**) have the lowest solid-state PL quantum yield, 2−3% (Table 2). These correspond to the bis(phenylene)-vinylene (**3d**) and 2,5-thienylene (**3f**) linked polyquino-

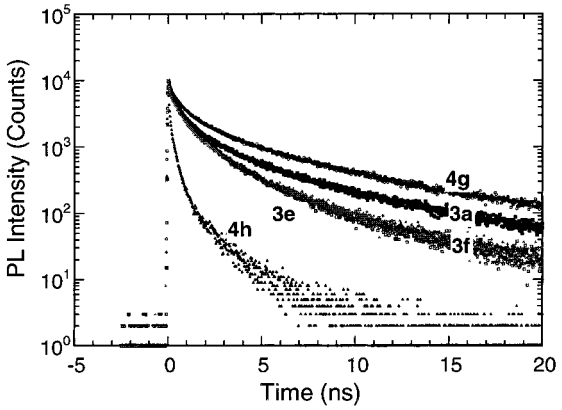

Figure 5. Fluorescence decay dynamics of thin films of polyquinolines: BuM-PPQ (**4h**), PDMPQ (**3e**), Bu-PPQ (**4g**), PPPQ (**3a**), and PTPQ (**3f**). The polymers were excited at 350 nm, and the emission was monitored at the PL peak of each polymer.

lines. The approximately factor of 3 reduction in PL emission efficiency of **3d** relative to **3a**−**c** is unclear but may be due to luminescence quenching arising from photooxidation of the vinylene linkage given the age of the polymer sample (over 3 years) and the fact that all the thin film processing and photophysical measurements were done under ambient laboratory air.[3] In the case of PTPQ, the small emission quantum yield may be largely because of the dominant effect of intramolecular charge transfer (ICT) between the bis(quinoline) and thiophene rings. Lending credence to this interpretation is the fact that the PL emission efficiency of a related thiophene-linked polyquinoxaline is about 2 orders of magnitude less than PTPQ;[5d] ICT is stronger in thiophene−quinoxaline chains than thiophene−quinoline materials because the quinoxaline ring is a stronger electron acceptor than the quinoline ring.

Since an integrating sphere was not used to measure the solid-state PL quantum efficiencies in Table 2, they are not absolute values but good lower bound estimates of the absolute quantities.[21] More importantly, the PL quantum yield data provide an excellent basis for comparing the series of polyquinolines as emissive materials for LEDs. The variation of PL quantum efficiency between 2 and 30% among the series of polyquinolines is interesting in revealing the effects of molecular and supramolecular structures on the luminescence efficiency. Since the EL device quantum efficiency (ϕ_{EL}) in organic LEDs is directly proportional to the PL quantum yield (ϕ_{PL}), $\phi_{EL} = f\gamma\phi_{PL}$ where f is the efficiency of exciton generation from electron−hole combination and γ is the charge injection efficiency,[1b] this suggests that a similar correlation of molecular and supramolecular structures with EL properties of the polyquinolines may be possible. However, charge injection and transport processes in the polymer LEDs may also vary substantially in the series of polyquinolines depending on the highest occupied molecular orbital (HOMO) and lowest unoccupied molecular orbital (LUMO) levels. Therefore, to better understand how the various factors influence the electroluminescence of the polyquinolines, it is necessary to know the HOMO/LUMO levels of the series of polymers and to fabricate and evaluate LEDs under identical conditions. Results of such studies will be discussed in subsequent sections.

Fluorescence Decay Dynamics. Figure 5 shows representative PL decay curves for BuM-PPQ (**4h**), PDMPQ (**3e**), Bu-PPQ (**4g**), PPPQ (**3a**), and PTPQ (**3f**). It was found that the PL decay dynamics of all the polyquinolines, except for **4h** and **4i**, can best be described by three-term exponential functions with one dominant lifetime. The best fit three lifetimes and their amplitudes for each polymer are given in Table 3. The multiple lifetimes needed to describe the PL decay dynamics of the polyquinolines suggest the existence of more than one excited-state species or the occurrence of various excited-state processes. We suggest that all the PL decay data are consistent with features of aggregation and excimer formation already observed from the steady-state PL data. The dominant PL lifetimes of **1**, **2**, **3a**−**f**, and **4g** are in the range of 2.42 ns for PTPQ (**3f**) to 5.22 ns for Bu-PPQ (**4g**). These excited-state lifetimes are unusually long compared to those of other luminescent conjugated polymers which typically have dominant lifetimes on the order of 100−600 ps.[17a,22]

Table 3. PL Decay Dynamics of Polyquinoline Thin Films

polymer	τ_1, ns	τ_2, ps	τ_3, ps	amplitude, % $\tau_1/\tau_2/\tau_3$
1, PPQ	4.72	1119	193	62.6/29.5/7.9
2, Bu-PQ	4.87	1160	170	67.0/27.0/6.0
3a, PPPQ	4.29	960	130	56.5/31.1/12.4
3b, PBPQ	3.13	694	107	65.5/24.3/10.2
3c, PBAPQ	4.55	956	125	53.4/30.2/16.4
3d, PSPQ	3.35	734	90	36.1/32.9/31.0
3e, PDMPQ	3.06	800	127	45.9/41.3/12.8
3f, PTPQ	2.42	718	106	50.3/36.0/13.7
4g, Bu-PPQ	5.22	1080	170	69.0/24.1/6.9
4h, BuM-PPQ	1.53	260	40	15.3/30.3/54.4
4i, BuN−PPQ	1.80	410	60	18.2/25.7/56.1

The dominant PL lifetimes of BuM-PPQ (**4h**) and BuN-PPQ (**4i**) are only 40 and 60 ps, respectively (Table 3). The dramatically shortened lifetimes of **4h** and **4i** compared to those of all the other polyquinolines confirm the fundamental difference observed in the steady-state emission properties between these two polymers and the remaining polyquinolines. In particular, the shortened lifetimes are very consistent with J-like aggregation of the chromophores.[23]

From the PL quantum efficiencies (Table 2) and measured lifetimes (τ) of the polyquinolines (Table 3), the excited-state decay rate constants (the radiative rate constant k_r and nonradiative rate constant k_{nr}) can be estimated.[22a,24] For example, PPPQ (**3a**) with 10% PL quantum efficiency and dominant lifetime of 4.29 ns has a $k_r \sim 2 \times 10^7$ s^{-1} and $k_{nr} \sim 2 \times 10^8$ s^{-1}. Except for **4h** and **4i** the radiative rate constant was of order 10^7−10^8 s^{-1} and the nonradiative rate constant was of order 10^8−10^9 s^{-1} for all the polyquinolines. The radiative and nonradiative rate constants for **4h** and **4i** were of order 10^9 and 10^{10} s^{-1}, respectively. These estimates show that the polyquinolines forming ground-state aggregates (**4h** and **4i**) have both enhanced emission and nonradiative decay rates compared to those forming excimers. How to reduce the nonradiative rate while preserving the enhanced emission rate in such aggregates of conjugated polymers remains a challenge that must be addressed through molecular and supramolecular engineering strategies.

B. Redox Properties and Electronic Structures. Charge injection processes and the associated electronic states of conjugated polymer thin films which are important for understanding EL devices can be readily investigated by electrochemical techniques, especially cyclic voltammetry. We have previously used cyclic voltammetry (CV) to study the redox properties of n-type

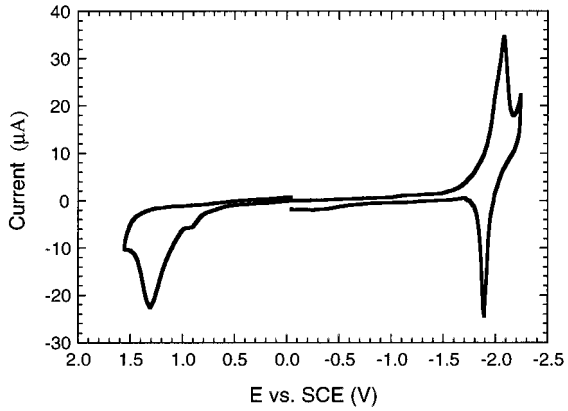

Figure 6. Cyclic voltammogram of Bu-PQ (**2**) in 0.1 M Bu_4NPF_6/acetonitrile at the scan rate of 20 mV/s.

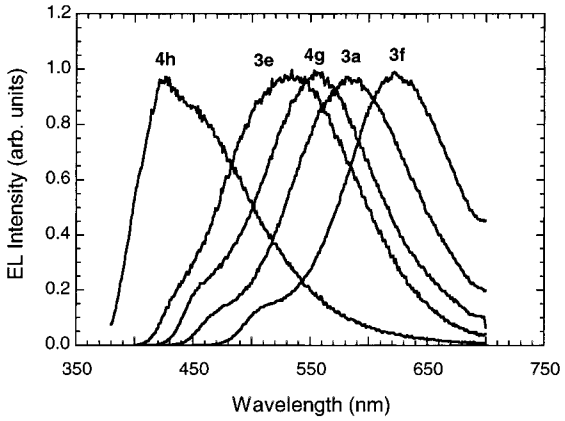

Figure 7. Representative EL spectra of polyquinolines: BuM-PPQ (**4h**), PDMPQ (**3e**), Bu-PPQ (**4g**), PPPQ (**3a**), and PTPQ (**3f**) at the turn-on voltage of each device.

conjugated polymers and estimate their HOMO/LUMO levels,[25] including the redox properties and electronic structures of the polyquinolines **1** and **3a**−**f**.[9] However, the electrochemical properties of the recently synthesized polyquinolines **2** and **4g**−**i** have not previously been reported. To better understand the electronic structures of these polymers in relation to charge injection characteristics in LEDs, we performed CV measurements on polymers **2** and **4g**−**i**. Figure 6 shows the reduction and oxidation CVs of Bu-PQ (**2**). The onset reduction and oxidation potentials of Bu-PQ (**2**) were found to be −1.86 and 0.78 V vs SCE, respectively. These values are almost the same as those of PPQ (**1**) (Table 1). Similar to other polyquinolines, Bu-PQ (**2**) showed a reversible reduction and an irreversible oxidation, indicating that the polyquinolines are intrinsic n-type (electron transport) semiconducting polymers. To facilitate easy comparison, the redox potentials for **4g**−**i** are collected in Table 1 together with those for the already reported polyquinolines.[9] Additional data on the redox properties of the polyquinolines, including formal potentials ($E^{o\prime}$) and peak potentials, can be found in a previous report.[9]

The *tert*-butyl substitution did not cause a significant change in the electrochemical properties of Bu-PQ (**2**) compared to PPQ (**1**). However, Bu-PPQ (**4g**) showed a more positive reduction potential (−1.58 V) compared to that of PPPQ (**3a**) (−1.90 V). The reason for the increase in reduction potential due to the *tert*-butyl substitution is not clear. Polymers **3a**−**e** exhibited similar redox properties, having reduction potentials of −1.90 to −2.04 V and oxidation potentials of 0.95 to 1.09 V. BuM-PPQ (**4g**) and BuN-PPQ (**4i**) have reduction potentials that are similar to those of **3a**−**e** but have more positive oxidation potentials. Polymer **3f** (PTPQ) showed a reversible reduction and a quasi-reversible oxidation,[9] indicating that PTPQ (**3f**) also exhibits some p-type (hole transport) semiconducting properties which may originate from its intramolecular charge-transfer characteristics.[19]

The ionization potential (IP) and electron affinity (EA) or their associated HOMO and LUMO energy levels can be estimated from the onset redox data in Table 1: IP/HOMO = E^{ox} + 4.4 eV and EA/LUMO = E^{red} + 4.4 eV, where the SCE energy level of −4.4 eV below the vacuum level is used.[9] Accordingly, the EA/LUMO energy level varies from 2.36 eV for PDMPQ (**3e**) to 2.82 eV for Bu-PPQ (**4g**), and the IP/HOMO energy level varies from 5.75 eV for BuM-PPQ (**4h**) to 5.18 eV for Bu-PQ (**2**). If, however, an SCE energy level of −4.8 eV relative to vacuum is used as the reference as done by others,[26] the EA and IP values would increase to 2.78−3.22 eV and 5.58−6.15 eV, respectively. The reversible electrochemical reduction of all the polyquinolines and their moderately high electron affinities suggest that good electron injection and transport could be achieved in LEDs. On the other hand, hole injection and transport could likely be more difficult because of the irreversible oxidation CV and quite high ionization potentials of the polyquinolines.

C. Electroluminescence. Either electroluminescence of the polyquinolines in single-layer ITO/polyquinoline/Al type devices was not feasible at all or the EL emission was extremely weak. Therefore, we focused our study on the ITO/HTL/polyquinoline/Al device structure where the hole-transport layer (HTL) is either TAPC:PS or PVK (see Figure 1). The hole-transport layer was 50 nm thick, and the polyquinoline layer was in the range 30−60 nm. Figure 7 shows representative EL spectra of the polyquinolines, showing that they exhibit different emission colors ranging from blue to green, yellow, orange, and red. Thus, by incorporating different linkages in the main chain or through side-group substitutions, the EL emission color of the polyquinolines can be tuned. BuM-PPQ (**4h**) with *tert*-butyl and methyl substitutions emits blue light. The nonconjugated PDMPQ (**3e**) with bis(phenylene)methylene linkage which disrupts the backbone conjugation generates green light. Bu-PPQ (**4g**) with the *tert*-butyl group gives yellow color. PTPQ (**3f**) with the thiophene linkage emits red light. PPPQ (**3a**) and other polyquinolines including **1**, **2**, and **3b**−**d** give orange color. EL spectra of the polyquinolines were found to be identical to their PL spectra as exemplified in Figure 2 for PPQ (**1**). This suggests that the EL emission from these ITO/HTL/polyquinoline/Al devices comes from the polyquinoline layer only and that the electroluminescence and photoluminescence of the polyquinolines originate from the same excited states that were previously identified as excimers and aggregates.

Figure 8 shows the current−voltage and luminance−voltage characteristics of PPQ (**1**) and Bu-PPQ (**4g**) EL devices. The ITO/TAPC:PS(50 nm)/PPQ(30 nm)/Al device had a turn-on voltage of 7 V and a luminance of 130 cd/m^2 at 17.5 V and a current density of 235 mA/cm^2. The ITO/TAPC:PS(50 nm)/Bu-PPQ(50 nm)/Al device showed bright yellow color emission with luminance of 280 cd/m^2 at a current density of 100 mA/cm^2. From similar current−voltage and luminance−voltage curves

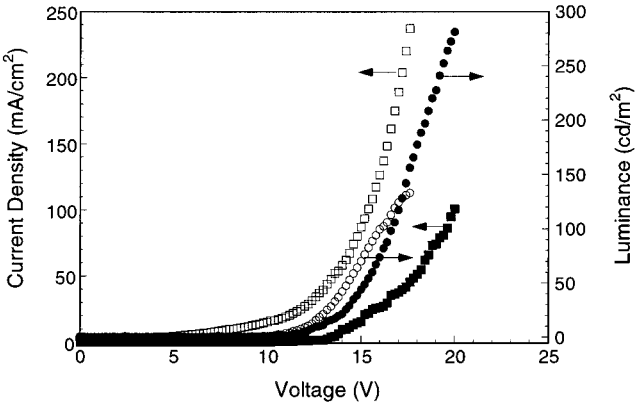

Figure 8. Current−voltage and luminance−voltage characteristics of LEDs fabricated from PPQ (**1**) (open marks) and Bu-PPQ (**4g**) (filled marks).

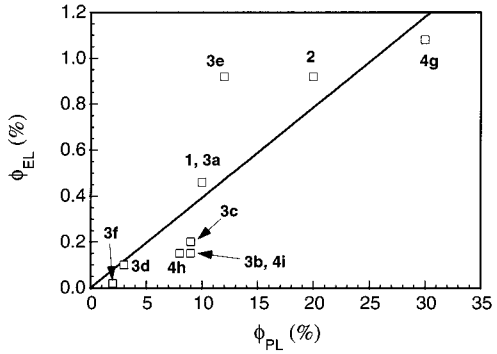

Figure 9. Dependence of EL device efficiency on PL quantum yield of the polyquinolines.

the turn-on voltages of all the polyquinoline LEDs were found to be essentially the same, 7−9 V, except for PTPQ (**3f**) which was 5 V and BuM-PPQ (**4h**) and BuN-PPQ (**4i**) which were 10−11 V (Table 2). After normalization by the device film thickness the turn-on electric field was the same for all the polyquinolines (∼8 × 10^5 V/cm) except for **3f** (5.6 × 10^5 V/cm) and **4h** and **4i** (1.2 × 10^6 V/cm). The higher turn-on electric field of **4h** and **4i** diodes is due largely to hole injection difficulty. We infer this from the fact that ITO/TAPC:PS/**4h**/Al and ITO/TAPC:PS/**4i**/Al diodes did not emit light whereas ITO/PVK/**4h**/Al and ITO/PVK/**4i**/Al diodes generated blue light. This indicates that hole injection from TAPC into these two polyquinolines was more difficult than from PVK (HOMO/LUMO = 5.8/2.3 eV).[27] The lower than average turn-on electric field of PTPQ (**3f**) diodes is due to the ready injection of holes from TAPC (HOMO/LUMO = ∼5.3/1.8 eV)[28] into PTPQ (HOMO/LUMO = 5.27/2.56 eV). These results suggest that the 7−9 V turn-on voltages of nearly all the polyquinoline LEDs and even other device performance characteristics (luminance, EL efficiency) could be substantially improved by finding an optimum hole-transport layer.

The polyquinoline EL diodes had luminance or brightness of 7−280 cd/m^2 and internal EL quantum efficiencies in the range of 0.02% for the red-light-emitting PTPQ (**3f**) to 1.08% for Bu-PPQ (**4g**) (Table 2). A most remarkable feature of the EL efficiency (ϕ_{EL}) data for the series of polyquinolines is that they approximately track the photoluminescence quantum efficiency (ϕ_{PL}) (Figure 9) and its variation with molecular structure. For example, except for a few cases, the ratio of ϕ_{PL} to ϕ_{EL} is on the order of 10−40 for the series of polyquinolines. Since $\phi_{EL} = f\gamma\phi_{PL}$ as pointed out earlier, these

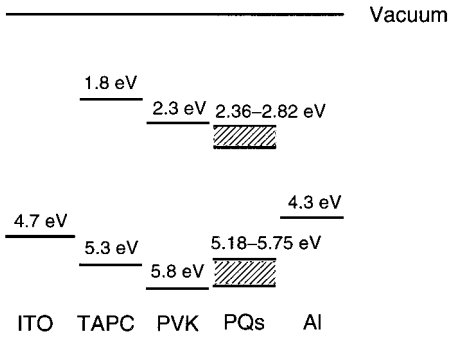

Figure 10. HOMO/LUMO levels of the polyquinolines (PQs), TAPC, and PVK in relation to the work function of the LED electrodes.

results suggest that the charge injection and transport processes as well as exciton generation from charge recombination are very similar in all the polyquinoline LEDs despite the large variation in electronic structure and particularly IP/HOMO and EA/LUMO levels. We understand this to imply that having a series of structurally related emissive semiconducting polymers can allow one to simultaneously optimize the materials (e.g., ϕ_{PL}) and device engineering (e.g., the product $f\gamma$) in polymer LEDs.

Another important implication of the previously discussed similarity of the turn-on electric fields of these polyquinoline LEDs and the approximate scaling of EL efficiency data with the PL quantum yields is that variation of the EA/LUMO energy levels by ∼0.5 eV among the series of polyquinolines does not appear to directly influence either the turn-on electric field or EL efficiency. Also, although there was a large barrier of ∼1.5−1.9 eV to electron injection from the aluminum electrode into the polyquinolines (Figure 10), yet good EL efficiency, moderate luminance, and efficient electron injection were obtained. In fact, the barrier to electron injection is comparable in size to that in ITO/PPV/Al single-layer diodes (PPV HOMO/LUMO = 5.1/2.71 eV) which have extremely poor efficiency.[1,5d] We propose that reaction at the aluminum/polyquinoline interface dominates the electron injection process in these polyquinoline LEDs. Formation of such an aluminum/polyquinoline complex could explain all the experimental data, particularly why all the polyquinolines, regardless of their EA/LUMO levels, have efficient electron injection. Although we do not have direct evidence of the Al/polyquinoline interface reaction, extensive surface spectroscopic studies of other metal/conjugated polymer interfaces suggest the generality of such reactions which are especially facilitated by the presence of electron-rich atoms in the polymers.[29] Our own prior studies of various heterocyclic polymers, including the polyquinolines, have established the facile coordination complexation of metal halide Lewis acids (e.g., $AlCl_3$) to the heteroatom sites.[11b,30] Similar Al atom complexation reaction starting at the imine nitrogen sites can be expected during evaporative deposition of Al onto polyquinoline thin films. Direct evidence of the proposed aluminum/polyquinoline interface reaction in these LEDs should be obtained in the future by X-ray photoelectron spectroscopy (XPS) and ultraviolet photoelectron spectroscopy (UPS).

Conclusions

Regulation of the molecular and supramolecular structures of the polyquinolines has allowed both the

photoluminescence and electroluminescence colors and efficiencies to be tuned over a wide range. Emission from thin films of the polyquinolines is characterized by primarily excimers with long excited-state lifetimes of 2.4−5.2 ns and fairly good photoluminescence quantum efficiencies of 2−30%. Electroluminescence diodes of the type ITO/HTL/polyquinoline/Al have quantum yields of up to 1% photons/electron and luminance levels of up to 280 cd/m^2. The light-emitting diodes fabricated from these emissive n-type conjugated polymers appear to be currently limited largely by hole injection and transport. The efficient electron injection from aluminum into the polyquinolines in these EL devices is proposed to be mediated by a reaction at the aluminum/polyquinoline interface which obviates the otherwise large energetic barrier to electron injection.

Acknowledgment. This work was supported by the Office of Naval Research and the National Science Foundation (CTS-9311741, CHE-9120001).

References and Notes

(1) Recent reviews: (a) Kraft, A.; Grimsdale, A. C.; Holmes, A. B. *Angew. Chem., Int. Ed. Engl.* **1998**, *37*, 402−428. (b) Friend, R. H.; Gymer, R. W.; Holmes, A. B.; Burroughes, J. H.; Marks, R. N.; Taliani, C.; Bradley, D. D. C.; dos Santos, D. A.; Bredas, J. L.; Logdlund, M.; Salaneck, W. R. *Nature* **1999**, *397*, 121−128.

(2) (a) Berggren, M.; Inganas, O.; Gustafsson, G.; Rasmusson, J.; Anderson, M. R.; Hjertberg, T.; Wennerstrom, O. *Nature* **1994**, *372*, 444−446. (b) Bai, X.; Holdcroft, S. *Macromolecules* **1993**, *26*, 4457−4460.

(3) Papadimitrakopoulos, F.; Yan, M.; Rothberg, L. J.; Katz, H. E.; Chandross, E. A.; Galvin, M. E. *Mol. Cryst. Liq. Cryst.* **1994**, *256*, 663−669.

(4) (a) Antoniadis, H.; Abkowitz, M. A.; Hsieh, B. R. *Appl. Phys. Lett.* **1994**, *65*, 2030−2032. (b) Blom, P. W. M.; de Jong, M. J. M.; Vleggaar, J. J. M. *Appl. Phys. Lett.* **1996**, *68*, 3308−3310. (c) Kreyenschmidt, M.; Klaerner, G.; Fuhrer, T.; Ashenhurst, J.; Karg, S.; Chen, W. D.; Lee, V. Y.; Scott, J. C.; Miller, R. D. *Macromolecules* **1998**, *31*, 1099−1103.

(5) (a) Greenham, N. C.; Moratti, S. C.; Bradley, D. D. C.; Friend, R. H.; Holmes, A. B. *Nature* **1993**, *365*, 628−630. (b) Jenekhe, S. A.; Zhang, X.; Chen, X. L.; Choong, V.-E.; Gao, Y.; Hsieh, B. R. *Chem. Mater.* **1997**, *9*, 409−412. (c) Zhang, X.; Jenekhe, S. A. *Mater. Res. Soc. Symp. Proc.* **1998**, *488*, 539−544. (d) Cui, Y.; Zhang, X.; Jenekhe, S. A. *Macromolecules* **1999**, *32*, 3824−3826.

(6) Tunney, S. E.; Suenaga, J.; Stille, J. K. *Macromolecules* **1987**, *20*, 258−264.

(7) Wnek, G. E.; Wasserman, B.; Dresselhaus, M. S.; Tunney, S. E.; Stille, J. K. *J. Polym. Sci., Polym. Lett. Ed.* **1985**, *23*, 609−612.

(8) Abkowitz, M. A.; Stolka, M.; Antoniadis, H.; Agrawal, A. K.; Jenekhe, S. A. *Solid State Commun.* **1992**, *83*, 937−941.

(9) Agrawal, A. K.; Jenekhe, S. A. *Chem. Mater.* **1996**, *8*, 579−589.

(10) Sybert, P. D.; Beever, W. H.; Stille, J. K. *Macromolecules* **1981**, *14*, 493−502.

(11) (a) Agrawal, A. K.; Jenekhe, S. A. *Macromolecules* **1991**, *24*, 6806−6808. (b) Agrawal, A. K.; Jenekhe, S. A. *Chem. Mater.* **1992**, *4*, 95−104. (c) Agrawal, A. K.; Jenekhe, S. A. *Macromolecules* **1993**, *26*, 895−905. (d) Agrawal, A. K.; Jenekhe, S. A. *Chem. Mater.* **1993**, *5*, 633−640.

(12) (a) Agrawal, A. K.; Jenekhe, S. A.; Vanherzeele, H.; Meth, J. S. *J. Phys. Chem.* **1992**, *96*, 2837−2843. (b) Agrawal, A. K.; Jenekhe, S. A.; Vanherzeele, H.; Meth, J. S. *Chem. Mater.* **1991**, *3*, 765−768.

(13) (a) Parker, I. D.; Pei, Q.; Marrocco, M. *Appl. Phys. Lett.* **1994**, *65*, 1272−1274. (b) Kim, J. L.; Cho, H. N.; Kim, J. K.; Hong, S. I. *Macromolecules* **1999**, *32*, 2065−2067.

(14) (a) Zhang, X.; Shetty, A. S.; Jenekhe, S. A. *Acta Polym.* **1998**, *49*, 52−55. (b) Shetty, A. S.; Zhang, X.; Jenekhe, S. A. *Mater. Res. Soc. Fall Meeting*, Boston, MA, Dec 1−5, 1997.

(15) Stille, J. K.; Parker, A.; Tsang, J.; Berry, G. C.; Featherstone, M.; Uhlmann, D. R.; Subramoney, S.; Wu, W.-L. In *Contemporary Topics in Polymer Science: Multiphase Macromolecular Systems*; Culberston, B. M., Ed.; Plenum Press: New York, 1989; Vol. 6, pp 43−60.

(16) Guilbault, G. G., Ed. *Practical Fluorescence*; Marcel Dekker: New York, 1990.

(17) (a) Osaheni, J. A.; Jenekhe, S. A. *J. Am. Chem. Soc.* **1995**, *117*, 7, 7389−7398. (b) Jenekhe, S. A.; Osaheni, J. A. *Chem. Mater.* **1994**, *6*, 1906−1909.

(18) Greenham, N.; Friend, R. H.; Bradley, D. C. C. *Adv. Mater.* **1994**, *6*, 491−494.

(19) (a) Shetty, A. S.; Liu, E. B.; Lachicotte, R. J.; Jenekhe, S. A. *Chem. Mater.* **1999**, *11*, 2292−2295. (b) Shetty, A. S.; Jenekhe, S. A. Manuscript in preparation.

(20) Jenekhe, S. A.; Osaheni, J. A. *Science* **1994**, *265*, 765−768.

(21) Greenham, N. C.; Samuel, I. D. W.; Hayes, G. R.; Philips, R. T.; Kessener, Y. A. R. R.; Moratti, S. C.; Holmes, A. B.; Friend, R. H. *Chem. Phys. Lett.* **1995**, *241*, 89−96.

(22) (a) Samuel, I. D. W.; Rumbles, G.; Collison, C. J. *Phys. Rev. B* **1995**, *52*, 11573−11576. (b) Osaheni, J. A.; Jenekhe, S. A.; Perlstein, J. *J. Phys. Chem.* **1994**, *98*, 12727−12736. (c) Osaheni, J. A.; Jenekhe, S. A. *Macromolecules* **1994**, *27*, 739−742.

(23) Kobayashi, T., Ed. *J-Aggregates*; World Scientific: Singapore, 1996.

(24) Since $\phi_{PL} = k_r/(k_r + k_{nr})$ and $\tau = 1/(k_r + k_{nr})$, the two unknowns can be obtained.

(25) (a) Yang, C.-J.; Jenekhe, S. A. *Macromolecule* **1995**, *28*, 1180−1196. (b) Chen, X. L.; Jenekhe, S. A. *Macromolecule* **1997**, *30*, 1728−1733. (c) Osaheni, J. A.; Jenekhe, S. A. *Chem. Mater.* **1995**, *7*, 672−682.

(26) Jandke, M.; Strohriegl, P.; Berleb, S.; Werner, E.; Brutting, W. *Macromolecules* **1998**, *31*, 6434−6443.

(27) Hamaguchi, M.; Yoshino, K. *Jpn. J. Appl. Phys.* **1996**, *35*, 4813−4818.

(28) Lin, L.-B.; Young, R. H.; Mason, M. G.; Jenekhe, S. A.; Borsenberger, P. M. *Appl. Phys. Lett.* **1998**, *72*, 864−866.

(29) Salaneck, W. R.; Strafstrom, S.; Bredas, J.-L. *Conjugated Polymer Surfaces and Interfaces;* Cambridge University Press: Cambridge, 1996.

(30) (a) Jenekhe, S. A.; Johnson, P. O. *Macromolecules* **1990**, *23*, 4419−4429. (b) Jenekhe, S. A.; Johnson, P. O.; Agrawal, A. K. *Macromolecules* **1989**, *22*, 3216−3222.

MA990960+